Distribution of Mahogany/Attractin mRNA in the rat central nervous system

Xin-Yun Lu[a,*], Teresa M. Gunn[b], Kun-Ruey Shieh[a], Gregory S. Barsh[b], Huda Akil[a], Stanley J. Watson[a]

[a] *University of Michigan School of Medicine, Mental Health Research Institute, 205 Zina Pitcher Place, Ann Arbor, MI 48109-0720, USA*
[b] *Departments of Pediatrics and Genetics, Howard Hughes Medical Institute, Stanford, CA 94305, USA*

Received 27 September 1999

Abstract The Mahogany/Attractin gene (*Atrn*) has been proposed as a downstream mediator of Agouti signaling because yellow hair color and obesity in *lethal yellow* (A^y) mice are suppressed by the *mahogany* ($Atrn^{mg}$) mutation. The present study examined the distribution of *Atrn* mRNA in the brain and spinal cord by in situ hybridization. *Atrn* mRNA was found widely distributed throughout the central nervous system, with high levels in regions of the olfactory system, some limbic structures, regions of the brainstem, cerebellum and spinal cord. In the hypothalamus, *Atrn* mRNA was found in specific nuclei including the suprachiasmatic nucleus, the supraoptic nucleus, the medial preoptic nucleus, the paraventricular hypothalamic nucleus, the ventromedial hypothalamic nucleus, and the arcuate nucleus. These results suggest a broad spectrum of physiological functions for the Atrn gene product.

Key words: Mahogany/Attractin; Agouti; Obesity; In situ hybridization; Brain; Spinal cord

1. Introduction

The *mahogany* mutation was originally identified as a modifier of *Agouti*, which encodes a paracrine signaling molecule that normally causes hair follicle melanocytes to make yellow pigment [1–3]. In rare gain-of-function *Agouti* mutations such as *lethal yellow* (A^y), ubiquitous expression of the Agouti protein causes non-pigmentary effects that include hyperphagia, increased body weight and linear growth and glucose intolerance (reviewed in [4]). The effects of A^y on both pigmentation and obesity are suppressed by the *mahogany* mutation [5–8], whereas obesity caused by the *fat* (Cpe^{fat}), *tubby* (*Tub*), *db* (*LepR*) or *Mc4r* mutations is not suppressed by the *mahogany* mutation [6]. Independent of interaction with A^y, Dinulescu et al. [8] have reported that the *mahogany* mutation causes hyperphagia and an increased metabolic rate in C57BL/6J mice.

Positional cloning recently identified *mahogany* as encoding a single transmembrane-spanning protein whose ectodomain is orthologous to a circulating human protein known as Attractin [6,7,9]. The mouse gene has recently been renamed *Attractin*, *Atrn*, and the *mahogany* mutation is referred to below as $Atrn^{mg}$.

Several observations suggest that *Atrn* may modulate signaling via melanocortin receptors, a family of G protein-coupled receptors first recognized by their ability to activate adenylate cyclase in response to Pro-opiomelanocortin (POMC) derivatives such as α-melanocyte stimulating hormone or adrenocorticotrophic hormone. The pigmentary effects of A^y are mediated by the melanocyte-specific melanocortin 1 receptor (MC1R), for which Agouti protein is an antagonistic ligand [10]. However, the body weight regulation effects of A^y are thought to be mediated centrally by the MC4R, a key regulator of feeding behavior that is expressed in many brain regions [11,12]. Loss-of-function mutations in *Mc1r* or *Mc4r* cause yellow pigmentation or obesity, respectively, very similar to the phenotypes caused by ubiquitous expression of Agouti in A^y mice. However, $Atrn^{mg}$ suppresses the effects of A^y but not those of the *Mc1r* or *Mc4r* mutations. In other words, *Atrn* is genetically downstream of A^y but genetically upstream of the *Mc1r* and *Mc4r*.

Except for the case of rare mutations such as A^y, Agouti protein is normally not expressed in the brain. Its ability to alter body weight regulation via the MC4R may represent an evolutionary artifact, since a homologous molecule, Agouti-related protein (Agrp), is normally expressed in the hypothalamus and is a potent antagonist of the MC4R [13,14]. Agrp mRNA is found mainly in the arcuate nucleus of the hypothalamus where its terminal fields closely parallel those of POMC [15,16].

The genetic interactions described above and the specificity with which $Atrn^{mg}$ suppresses Agouti-induced obesity implicate *Atrn* in a direct relationship with Agouti protein signaling. By contrast, the observations of Dinulecu et al. [8] suggest additional roles for *Atrn* in energy homeostasis. To better understand how *Atrn* controls body weight regulation, we have examined the neuroanatomical distribution of *Atrn* mRNA in the rat brain and spinal cord. If the ability of $Atrn^{mg}$ to suppress Agouti-induced obesity is mediated via the central melanocortinergic system, one would expect *Atrn* mRNA to be expressed in specific regions of the brain and to exhibit a pattern that overlaps with that of *Mc4r* mRNA. However, if *Atrn* acts via alternative mechanisms, one might expect its mRNA to be found in regions of the central nervous system independent of the melanocortinergic system. As described below, our results are consistent with both scenarios and point to *Atrn* as a pleiotropic regulator of energy homeostasis.

2. Materials and methods

2.1. Animals

Adult male Sprague-Dawley rats (300–350 g) were purchased from Charles River Laboratories. Food and water were available ad libitum. After a week of habituation, rats were killed by rapid decapitation. Brains were removed, frozen in isopentane (−40°C). Serial 20

*Corresponding author. Fax: (1) (734) 647-4130.
E-mail: xylu@umich.edu

PII: S0014-5793(99)01494-5

μm tissue sections were cut in a cryostat, thaw-mounted onto poly-lysine-subbed slides and stored at −80°C until in situ hybridization.

2.2. Preparation of riboprobes

Three Mahogany/Attractin cDNAs, corresponding to the most 3′ region of the 3′ untranslated region, upstream of the region encoding the transmembrane domain and downstream of the region encoding the transmembrane domain, respectively, were inserted into pBluescript plasmid. Plasmids containing subcloned Mahogany/Attractin cDNAs were linearized using *Not*I or *Eco*RI and used as templates to prepare RNA probes. To generate sense and antisense ^{35}S-labelled cRNA probes, the linearized plasmid was incubated at 37°C for 2 h in 20 μl reaction mixture consisting of 1×transcription buffer (BRL), 75 μCi [α-^{35}S]UTP (>1000 Ci/mmol, 20 mCi/ml; Amersham), 100 μCi [α-^{35}S]CTP (800 Ci/mmol, 40 mCi/ml), 150 μM ATP, 150 μM GTP, 10 mM dithiothreitol, 20 U RNase inhibitor and 6 U T7 or T3 RNA polymerase. The probes were separated from free nucleotides over a Sephadex G50/50 column.

2.3. Isotopic in situ hybridization

The tissue sections were removed from −80°C freezer, fixed in 4% paraformaldehyde for 1 h and rinsed twice in 2×SSC (300 mM sodium chloride, 30 mM sodium citrate, pH 7.2). The sections were then acetylated in 0.1 M triethanolamine, pH 8.0, with 0.25% acetic anhydride (10 min) and dehydrated through graded alcohol. ^{35}S-labelled cRNA probes were diluted to 2×10^6/70 μl in 50% hybridization buffer (50% formamide, 10% dextran sulfate, 3×SSC, 50 mM sodium phosphate buffer, pH 7.4, 1×Denhart's solution, 0.1 mg/ml yeast tRNA and 30 mM DTT). Diluted probes (70 μl) were placed on each slide and the sections were coverslipped. Hybridization was performed in an incubator at 55°C for 16 h. After incubation, coverslips were lifted with 2×SSC, rinsed three times in 2×SSC, then incubated in RNase A (200 μg/ml) for 1 h at 37°C, followed by a wash sequence: 2×SSC, 1×SSC, 0.5×SSC and 0.1×SSC (5 min each at room temperature). Finally, the sections were washed in 0.1×SSC at 70°C for 1 h, then rinsed in distilled water and dehydrated in a graded series of alcohols. Sections were exposed to X-ray film (Kodak BioMax MR) and then dipped in Kodak NTB2 autoradiography emulsion. The specificity of in situ hybridization signals was assured by (1) hybridizing tissue sections with three antisense probes generated to different regions of the Mahogany/Attractin gene, (2) incubating sections with three sense strand probes or (3) pretreating the tissue with RNase (200 μg/ml at 37°C for 60 min) prior to hybridization with antisense probes. The autoradiographic images from the films or emulsion were captured and analyzed with a MCID/M5 image analysis system (Imaging Research, Ont., Canada). Anatomical localization was verified according to the rat brain atlas [17,18].

3. Results and discussion

The distribution of *Atrn* mRNA in the central nervous system was examined using in situ hybridization with cRNA probes. The specificity of in situ hybridization results was determined in several ways. First, hybridization with three antisense probes directed against the different regions of the *Atrn* gene produced identical labelling patterns at all levels of the neuroaxis. Second, no hybridization signals were detected using either sense probes or RNase pretreatment. The specificity of the riboprobe used for mapping in the present study is illustrated in Fig. 1. Figs. 2 and 3 show representative autoradiograms of different brain areas and spinal cord expressing *Atrn* mRNA, which is widely distributed but discretely located throughout the rat central nervous system. Nissl counterstaining of the tissue sections demonstrated that *Atrn* mRNA was expressed in the neurons and not in glial cells (Fig. 3A′).

We observed *Atrn* mRNA in several regions of the hypothalamus (Table 1 and Fig. 2), an important structure for the control of energy intake and energy expenditure. Low to moderate levels of mRNA were observed in the ventromedial hypothalamic nucleus and arcuate nucleus. However, the most robust labelling within the hypothalamus was observed in the suprachiasmatic nucleus. This nucleus, together with two connected regions, the paratenial thalamic nucleus and pineal gland (both containing *Atrn* mRNA), is believed to serve as a major pacemaker for circadian rhythms such as pituitary adrenal function, body temperature and feeding [19]. *Atrn* mRNA was also observed in the paraventricular nucleus and supraoptic nucleus, suggesting a potential role in the regulation of posterior pituitary gland function. Finally, *Atrn* mRNA was present in the preoptic nucleus, which is a key structure in thermoregulation.

The primary olfactory cortices contain high levels of *Atrn* mRNA. Strong labelling was observed in the piriform cortex, tenia tecta, anterior olfactory nucleus, olfactory tubercle and entorhinal cortex (Table 1 and Fig. 2). These olfactory structures have been implicated in cognition and taste/visceral integration. The efferent projections from these regions terminate heavily in the lateral hypothalamic area [20], the feeding center, suggesting a potential role for *Atrn* in translating taste/visceral signals into feeding behavior. *Atrn* mRNA shows extensive distribution in other forebrain limbic areas as well. For example, very intense labelling was observed in the CA1-3 Ammon's horn and the dentate gyrus of the hippocampal formation. Moderate levels of *Atrn* mRNA expression were observed in the prefrontal cortex, anterior limbic cortex and cingulate gyrus. *Atrn* mRNA was also present in some limbic subcortical structures including amygdala, lateral septum and habenula. In general, these limbic cortical and subcortical regions are believed to play a role in fear, aggression, stress, learning and memory. In addition, high levels of *Atrn* mRNA were detected in areas known to subserve mechanisms underlying positive reinforcement, including the substantia nigra, ventral tegmental area, raphe nucleus, locus coeruleus.

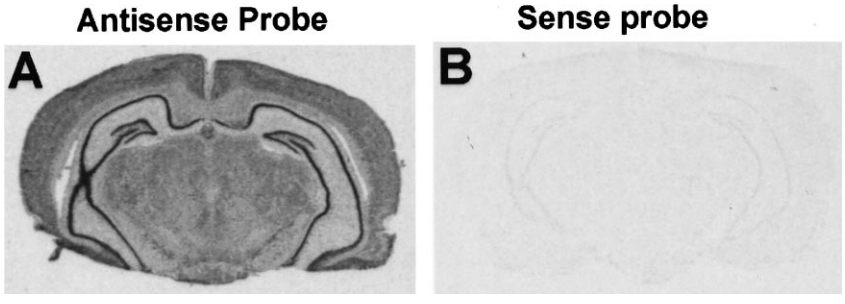

Fig. 1. Photomicrographs from film autoradiograms illustrating the specificity of the Mahogany/Attractin cRNA probes. A: Hybridization with antisense probes. B: Hybridization with sense probes.

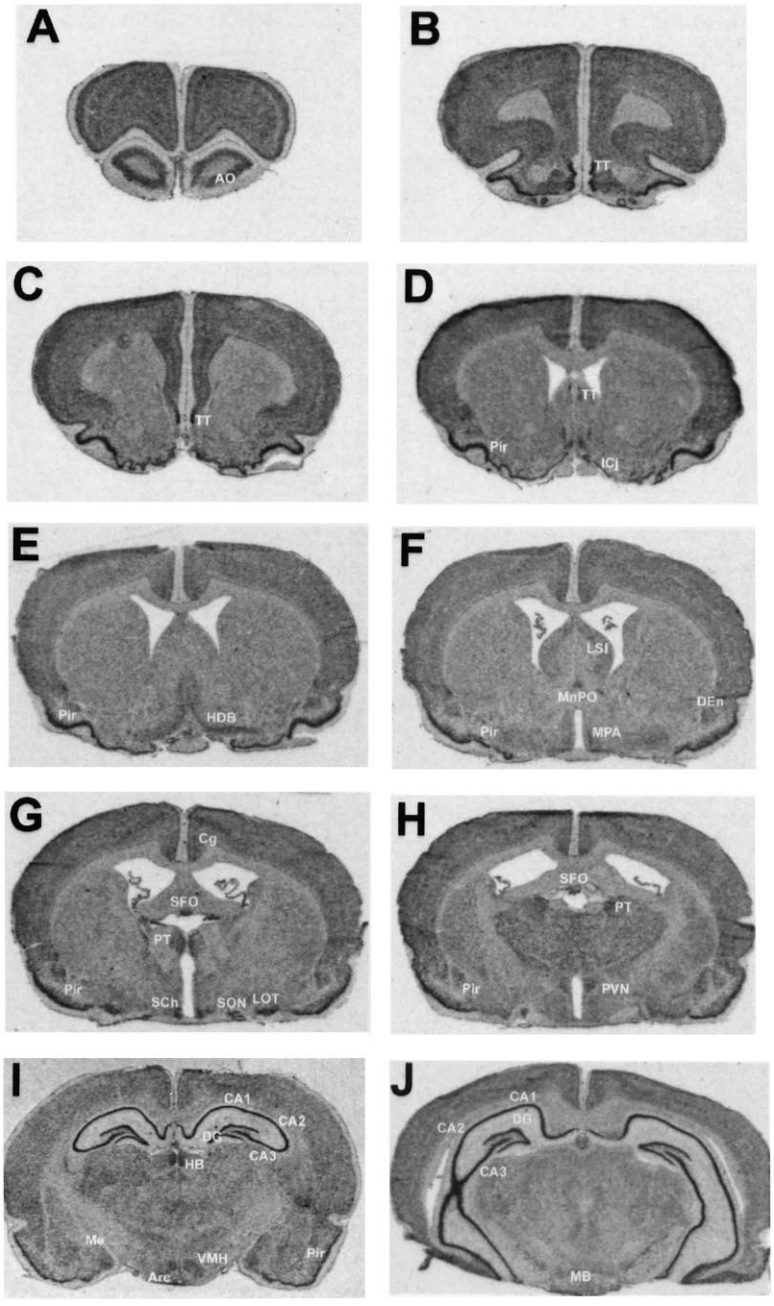

Fig. 2. A–P: Photomicrographs from film autoradiograms of a series of representative coronal brain sections arranged in a rostrocaudal sequence, illustrating regional localization of Mahogany/Attractin mRNA in the rat brain. AO, anterior olfactory nucleus; TT, tenia tecta; Pir, piriform cortex; ICj, islands of Calleja; LS, lateral septal nucleus; Cg, cingulate area; SFO, subfornical organ; PT, paratenial thalamic nucleus; SCH, suprachiasmatic nucleus; SON, supraoptic nucleus; LOT, nucleus lateral olfactory tract; Me, medial amygdala; Hb, habenula; PVN, paraventricular nucleus; VMH, ventromedial hypothalamic nucleus; Arc, arcuate nucleus; Hb, habenular nucleus; CA1-3, hippocampus; DG, dentate gyrus; CG, central gray; SN, substantia nigra; RN, red nucleus; VTA, ventral tegmental area; Pg, pineal gland; DR, dorsal raphe nucleus; IP, interpeduncular nucleus; PBG, parabigeminal nucleus; VTg, ventral tegmental nucleus; Pn, pontine nucleus; DTg, dorsal tegmental nucleus; Mo5, motor trigeminal nucleus; A5, noradrenaline cells; LC, locus coeruleus; PB, parabrachial nucleus; Fn, facial nucleus; Sp5, spinal trigeminal nucleus; IO, inferior olive; Sol, solitary tract nucleus; RtN, reticular nucleus; MdRN, medullary reticular nucleus.

These nuclei represent the major cell groups of the dopaminergic, serotonergic and non-adrenergic systems.

Atrn mRNA is highly expressed in the areas involved in control of motor and balance control such as the cerebellum, inferior olivary nucleus and ventral horn of the spinal cord (Table 1, Figs. 2 and 3C,D). In the midbrain, *Atrn* mRNA is present in the red nucleus (Fig. 3A,A′), subthalamic nucleus and interpeduncular nucleus, which are believed to participate in coordination of voluntary movements through connections to the cerebellum, spinal cord and basal ganglion. Other motor areas that displayed high expression of *Atrn* mRNA included the oculomotor nucleus, the facial nucleus, the motor trigeminal nucleus and the hypoglossal nucleus.

Several sensory areas contain *Atrn* mRNA, including the nucleus of the solitary tract and parabrachial nucleus (Fig. 2). These regions receive taste/visceral inputs from the nodose

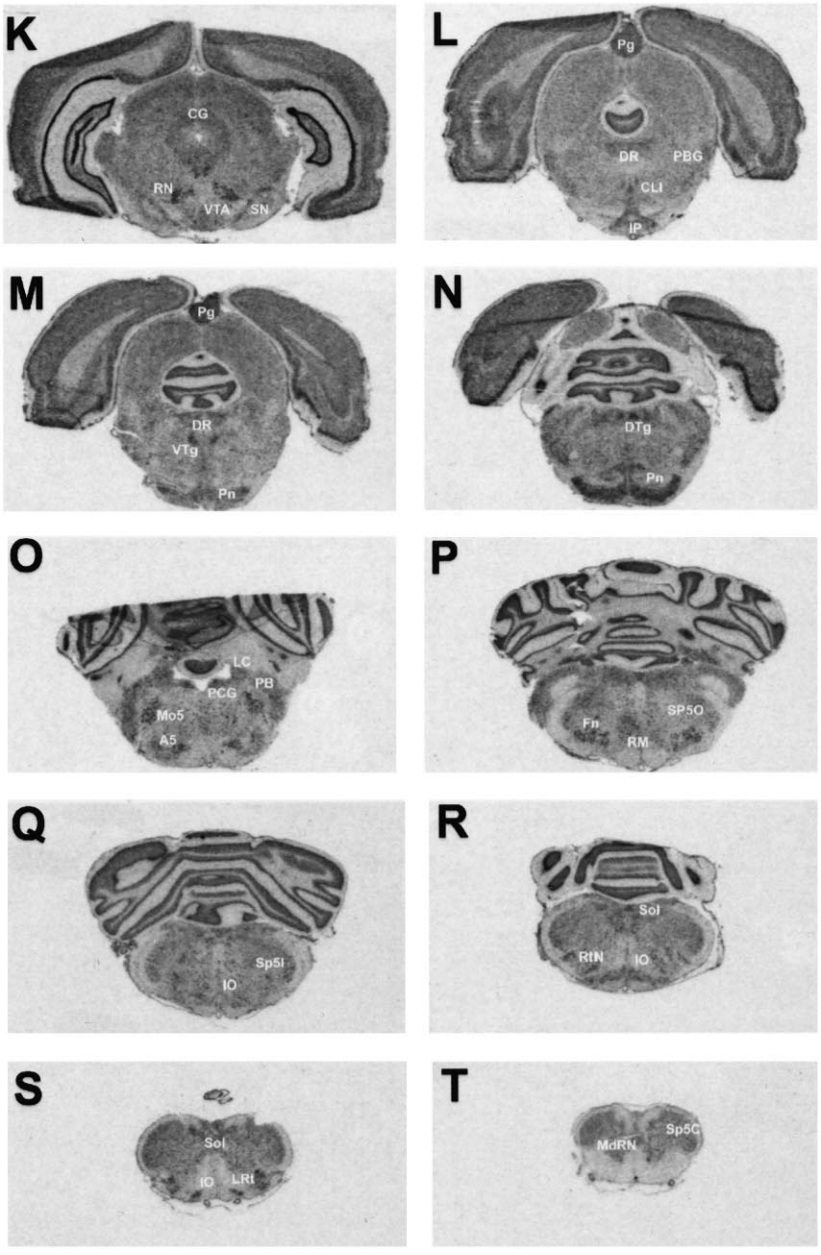

Fig. 2 (*continued*).

ganglion, suggesting a potential role for *Atrn* in modulating the flow of gustatory and visceral information. Interestingly, expression of *Atrn* mRNA was also seen in areas for pain modulation, such as the periaqueductal gray, nucleus raphe magnus, spinal trigeminal nucleus and dorsal horn of the spinal cord (Table 1). The periaqueductal gray and nucleus raphe magnus have been demonstrated to send direct and indirect projections to the nociceptive neurons in laminae I and II of the spinal dorsal horn [21,22].

Finally, we observed *Atrn* mRNA in laminae VII and X of the thoracic and lumbar spinal cord (Fig. 3D,D′), especially in the intermediolateral nucleus (Fig. 3D′), which provide sympathetic preganglionic neurons that regulate cardiovascular activity and brown adipose tissue thermogenesis. Alteration of one or both functions could account for the increased basal metabolic rate and hyperphagia observed by Dinulescu et al. [8] in $Atrn^{mg}/Atrn^{mg}$ mice.

The brain distribution of *Atrn* mRNA demonstrated by the present study points to the potential involvement of *Atrn* in multiple pathways of feeding and metabolism. Based on the genetic and molecular genetic studies, we [7] and others [6] have previously suggested that *Atrn* might function as a low-affinity receptor for Agouti protein and possibly Agrp. The present results do not refute this hypothesis, because *Atrn* mRNA is expressed in many regions of the brain that overlap with those of *Mc4r* mRNA. However, the overall pattern is quite different from the distribution of either *Mc4r* or Agrp terminal fields, especially when one considers the relative levels of expression. For example, *Atrn* mRNA is expressed at very high levels in the hippocampus, where *Mc4r* mRNA is very weak and Agrp terminal fields are absent. Conversely, the lateral hypothalamic area and dorsomedial hypothalamic nucleus are thought to be major effector sites of Agrp and Agouti protein with regard to body weight reg-

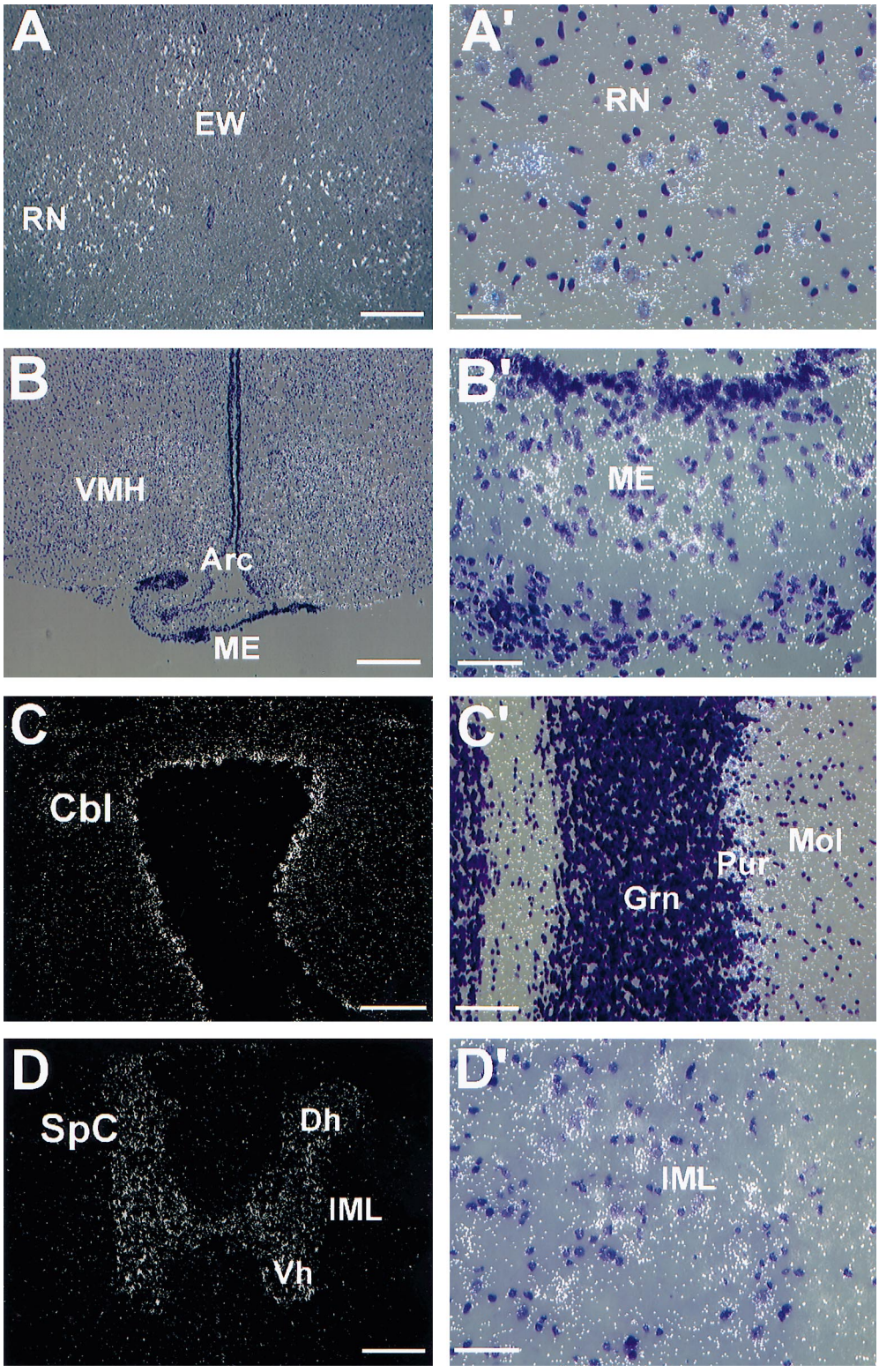

Fig. 3. Dark-field photomicrographs from emulsion autoradiograms (C and D) and photomicrographs of double exposures with dark-field (showing mRNA expression) and bright-field (showing cell staining) from Nissl counter-stained emulsion slides (A, A′, B, B′, C′ and D′). A and A′, red nucleus. B and B′, hypothalamus. ME, median eminence. C and C′, cerebellum. Mol, molecular layer; Pur, Purkinje cell layer; Grn, granular layer. D and D′, Spinal cord (SpC). Dh, dorsal horn; Vh, ventral horn; IML, intermidiolateral nucleus. Scale bars = 400 μm in A, B and D; 200 μm in C; 50 μm in A′, B′ and D′; 100 μm in C′.

ulation, yet expression of *Atrn* mRNA in these regions is relatively weak or absent. It should be noted that while the non-pigmentary effects of Agouti protein in A^y mice are almost certainly mediated via the MC4R, obesity in these animals is caused by ubiquitous expression of Agouti and could represent different effector sites than those normally utilized by endogenous Agrp. For example, *Mc4r* mRNA is expressed at high levels in the ventromedial hypothalamus, an area rel-

Table 1
Relative abundance of the Mahogany/Attractin mRNA in the rat nervous system

Forebrain	
Anterior olfactory nucleus	+++
Piriform cortex	++++
Olfactory tubercle	+++
Tenia tecta	+++
Entorhiral cortex	++
Islands of Calleja	++
Prefrontal cortex	++
Cingulate area	++
Anterior limbic cortex	+
Cerebral cortex	+
Dorsal endopiriform nucleus	++
Lateral septum	++
Horizontal limb diagonal band	+
Subfornical organ	++
Indusium griseum	+++
Hippocampal formation	
CA1	++++
CA2	++++
CA3	++++
Dentate gyrus	++++
Amygdala	+
Medial habenular nucleus	++
Paratenial thalamic nucleus	+
Central medial thalamic nucleus	++
Zona incerta	+
Subthalamic nucleus	++
Hypothalamus	
Medial preoptic area	+
Suprachiasmatic nucleus	++
Supraoptic nucleus	++
Paraventricular hypothalamic nucleus	+
Ventromedial nucleus	++
Arcuate nucleus	++
Median eminence	++
Mammilary nucleus	++
Pineal gland	+
Midbrain	
Substantia nigra	++
Ventral tegmental area	+
Interpeduncular nucleus	+
Red nucleus	++
Periaquaductal gray	+
Cerebellum	
Purkinje cell layer	+++
Granular layer	++
Pons and medulla	
Pontine nucleus	+++
Raphe nucleus	++
Locus coeruleus	++
Ventral tegmental nucleus	++
Dorsal tegmental nucleus	++
Parabigeminal nucleus	+
Parabrachial nucleus	++
Central gray pons	++
Noradrenaline cells	++
Motor trigeminal nucleus	++
Spinal trigeminal nucleus	+
Inferior olive	++
Reticular nucleus	++
Hypoglossal nucleus	++
Solitary tract nucleus	++
Spinal cord	
Dorsal horn	++
Intermediolateral nucleus	+++
Ventral horn	+++

The relative densities were estimated at a four-point scale: ++++ very strong labelling, +++ high density, ++ moderate density, + low density.

atively poor in Agrp terminal fields. Additional insight into these issues should come from biochemical studies of Atrn protein, Agouti protein and Agrp and from determining whether *Atrn*^{mg} can suppress obesity caused by ubiquitous expression of Agrp in transgenic mice.

The predicted Atrn protein resembles certain cell surface proteoglycans, some of which function as low-affinity receptors for a variety of soluble mediators. Because *Atrn* mRNA is found in discrete regions of the brain, it is not likely to subserve a 'housekeeping' role. The observations of Dinulescu et al. [8] suggest that *Atrn* controls the metabolic rate and feeding behavior independent of melanocortinergic signaling and the expression patterns described here provide a foundation for further investigating these hypotheses. For example, an increased basal metabolic rate in *Atrn*^{mg}/*Atrn*^{mg} mice could reflect a role for *Atrn* in regulation of sympathetic outflow, a question that could be investigated directly in tissue preparations of mutant mice. Finally, the high level of *Atrn* mRNA expression in areas of the limbic cortex and hippocampus suggests potential roles in complex behavior, including cognition, learning and memory. Thus, while the precise functions of the *Atrn* gene product remain speculative, the expression patterns described here provide a framework for generating and testing more refined hypotheses regarding the role of *Atrn* in the central nervous system.

Acknowledgements: This work was supported by a Grant from the University of Michigan GI center to S.J.W. (P30DK34933) and by Grants from the National Institutes of Health to S.J.W. and H.A. (MH42251) and to G.S.B. (DK28506). G.S.B. is an Associate Investigator of the Howard Hughes Medical Institute.

References

[1] Bultman, S.J., Michaud, E.J. and Woychik, R.P. (1992) Cell 71, 1195–1204.
[2] Lane, P.W. and Green, M.C. (1960) J. Hered. 51, 228–230.
[3] Miller, M.W., Duhl, D.M.J., Vrieling, H., Cordes, S.P., Ollmann, M.M., Winkes, B.M. and Barsh, G.S. (1993) Genes Dev. 7, 454–467.
[4] Jackson, I.J., Budd, P., Horn, J.M., Johnson, R., Raymond, S. and Steel, K. (1994) Pigment. Cell Res. 7, 73–80.
[5] Miller, K.A., Gunn, T.M., Carrasquillo, M.M., Lamoreux, M.L., Galbraith, D.B. and Barsh, G.S. (1997) Genetics 146, 1407–1415.
[6] Nagle, D.L., McGrail, S.H., Vitale, J., Woolf, E.A., Dussault Jr., B.J., DiRocco, L., Holmgren, L., Montagno, J., Bork, P., Huszar, D., Fairchild-Huntress, V., Ge, P., Keilty, J., Ebeling, C., Baldini, L., Gilchrist, J., Burn, P., Carlson, G.A. and Moore, K.J. (1999) Nature 398, 148–152.
[7] Gunn, T.M., Miller, K.A., He, L., Hyman, R.W., Davis, R.W., Azarani, A., Schlossman, S.F., Duke-Cohan, J.S. and Barsh, G.S. (1999) Nature 398, 152–156.
[8] Dinulescu, D.M., Fan, W., Boston, B.A., McCall, K., Lamoreux, M.L., Moore, K.J., Montagno, J. and Cone, R.D. (1998) Proc. Natl. Acad. Sci. USA 95, 12707–12712.
[9] Duke-Cohan, J.S., Gu, J., McLaughlin, D.F., Xu, Y., Freeman, G.J. and Schlossman, S.F. (1998) Proc. Natl. Acad. Sci. USA 95, 11336–11341.
[10] Ollmann, M.M., Lamoreux, M.L., Wilson, B.D. and Barsh, G.S. (1998) Genes Dev. 12, 316–330.
[11] Fan, W., Boston, B.A., Kesterson, R.A., Hruby, V.J. and Cone, R.D. (1997) Nature 385, 165–168.
[12] Huszar, D., Lynch, C.A., Fairchild-Huntress, V., Dunmore, J.H., Fang, Q., Berkemeier, L.R., Gu, W., Kesterson, R.A., Boston, B.A., Cone, R.D., Smith, F.J., Campfield, L.A., Burn, P. and Lee, F. (1997) Cell 88, 131–141.
[13] Ollmann, M.M., Wilson, B.D., Yang, Y.K., Kerns, J.A., Chen, Y., Gantz, I. and Barsh, G.S. (1997) Science 278, 135–138.

[14] Shutter, J.R., Graham, M., Kinsey, A.C., Scully, S., Luthy, R. and Stark, K.L. (1997) Genes Dev. 11, 593–602.
[15] Broberger, C., Johansen, J., Johansson, C., Schalling, M. and Hokfelt, T. (1998) Proc. Natl. Acad. Sci. USA 95, 15043–15048.
[16] Bagnol, D., Lu, X.-Y., Kaelin, C.B., Day, H.E.W., Ollmann, M., Gantz, I., Akil, H., Barsh, G.S. and Watson, S.J. (1999) J. Neurosci. Rapid Commun. (in press).
[17] Kruger, L., Saporta, S. and Swanson, L.W. (1995) Photographic Atlas of the Rat Brain, Cambridge University Press, New York.
[18] Paxinos, G. and Watson, C. (1986) The Rat Brain in Stereotaxic Coordinates, Academic Press, San Diego, CA.
[19] Abe, K., Kroning, J., Greer, M.A. and Critchlow, V. (1979) Neuroendocrinology 29, 119–131.
[20] Shipley, R.B. (1995) The Rat Nervous System, Academic Press, Sydney.
[21] Beitz, A.J. (1995) The Rat Nervous System, Academic Press, Sydney.
[22] Jones, B.E. (1995) The Rat Nervous System, Academic Press, Sydney.